Spectrochimica Acta Part A: Molecular and Biomolecular Spectroscopy 261 (2021) 120042

Contents lists available at ScienceDirect

Spectrochimica Acta Part A: Molecular and Biomolecular Spectroscopy

journal homepage: www.elsevier.com/locate/saa

A highly selective and sensitive Zn^{2+} fluorescent sensor based on zinc finger-like peptide and its application in cell imaging

Shuaibing Yu [a,1], Yan Li [a,1], Lei Gao [b], Peiran Zhao [b], Lei Wang [a], Lianzhi Li [a,*], Ying-Wu Lin [c,*]

[a] School of Chemistry and Chemical Engineering, Liaocheng University, Liaocheng, China
[b] Zhong Yuan Academy of Biological Medicine, Liaocheng People's Hospital Affiliated to Shandong University, Liaocheng, China
[c] School of Chemistry and Chemical Engineering, University of South China, Hengyang, China

HIGHLIGHTS

- A peptidyl ratiometric fluorescent sensor Dansyl-His-Gln-Arg-Thr-His-Trp-NH_2 was developed.
- The sensor exhibited a high selectivity and sensitivity for Zn^{2+} over other metal ions.
- The detection of Zn^{2+} was based on fluorescence resonance energy transfer principle.
- The sensor was successfully used for detection of Zn^{2+} in living HeLa cells.

GRAPHICAL ABSTRACT

A peptidyl ratiometric fluorescent sensor (Dansyl-His-Gln-Arg-Thr-His-Trp-NH_2) has been developed for highly selective and sensitive detection of Zn^{2+} over other common metal ions by fluorescence resonance energy transfer (FRET), as suggested by both experimental results and molecular modeling. The sensor was successfully used for detection of Zn^{2+} in living HeLa cells.

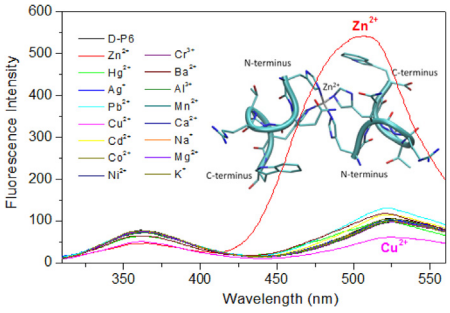

ARTICLE INFO

Article history:
Received 16 March 2021
Received in revised form 14 May 2021
Accepted 29 May 2021
Available online 2 June 2021

Keywords:
Fluorescence sensor
Peptide
Zn^{2+}
Fluorescent resonance energy transfer
Cell imaging

ABSTRACT

Developing new chemosensors for detection of Zn^{2+} has attracted great attentions because of the important roles of Zn^{2+} in biological systems, and it will produce toxic effects with an excessive intake of zinc ion. Metalloproteins are often used as an effective template for the design and development of peptide-based fluorescent sensors. In this study, we designed a new and simple ratiometric fluorescent sensor for Zn^{2+}, which was based on a zinc finger-like peptide and labeled with a dansyl group, i.e., Dansyl-His-Gln-Arg-Thr-His-Trp-NH_2 (D-P6), by using solid phase peptide synthesis (SPPS). The dimeric peptide has a high affinity for Zn^{2+} over other metal ions, as indicated by spectroscopic studies, as well as molecular modeling. Remarkably, the sensor exhibited a highly selective and sensitive ratiometric fluorescent response to Zn^{2+} by fluorescent resonance energy transfer effect between tryptophan residue and fluorophore dansyl group, with a very low detection limit of 33 nM in aqueous solution. Furthermore, the sensor displayed a very low biotoxicity, which allows successful detection of Zn^{2+} in living HeLa cells. We believe that the new sensor may have potential applications in biological science.

1. Introduction

Zinc is the second most abundant transition metal ion in the human body and plays important roles in many biological pro-

* Corresponding authors.
E-mail addresses: lilianzhi@lcu.edu.cn (L. Li), ywlin@usc.edu.cn (Y.-W. Lin).
[1] These authors contributed equally.

https://doi.org/10.1016/j.saa.2021.120042
1386-1425/

cesses, such as gene expression and apoptosis, metalloenzyme catalysis, immune function and neurotransmission [1–5]. Many pathological processes including Alzheimer's disease, ischemic stroke, infantile diarrhea and epilepsy are related to zinc [6–8]. However, zinc is a common contaminant in agricultural and food wastes [9], and excessive zinc ions may reduce the soil microbial activity and cause phytotoxic effects [10]. Therefore, it is of great importance for us to design and syntheze sensors for detection of zinc with high selectivity and sensitivity.

Fluorescence sensing, owing to its high sensitivity and selectivity, has become an attractive and ideal detection method [11–16]. Typically, fluorescent chemosensors consist of a receptor and a fluorophore, where the receptor is used for selective recognition and binding of metal ions and the fluorophore is mainly used for signal conversion, by transferring the recognition events into fluorescent signals [17–20]. Therefore, an ideal fluorescent sensor should meet two basic requirements. First, the receptor, the central processing unit of a sensor, must have a high affinity for the analyte (binding selectivity). Second, the fluorescence signal should not be quenched by the environment (signal selectivity) [21]. Up to now, considerable efforts have been devoted to the design of fluorescent chemosensors based on dansyl, fluorescein, quinoline, coumarin and naphthalimide, as well as peptides, for the detection of Zn^{2+} [22–35]. Meanwhile, most of these chemosensors have disadvantages, such as poor solubility in water, low selectivity or sensitivity, and the interference by Cd^{2+} that belongs to the same group in the periodic table with similar properties as Zn^{2+} [36–38]. Moreover, most reported fluorescent sensors display an increase or decrease in the emission intensity upon binding to species of interest.

Actually, the ratio between the two emission intensities can be used to determine the concentration of analytes and provide a built-in correction for environmental effects, such as photobleaching, sensor molecule concentration, the environment around the sensor molecule (pH, polarity, temperature, and so forth), and stability under illumination [3]. Therefore, ratiometric sensors for transition metal ions are more attractive, which make it possible to measure the analyte more accurately with minimal background signals [39]. In the last decade, chemists have focused on using chelating units of organic ligands to design fluorescent chemosensors. However, the procedure of synthesis was rigorous and the binding of ligand to metal ions was not always reversible [40,41].

Alternatively, we have recently reported several peptide-based sensors for the detection of Hg(II), Cu(II) and Cd(II) [42–47]. Our designs were based on the following rationales: (1) Peptide probes, consisting of natural amino acids, can be easily synthesized by fluorenylmethoxy-carbonyl(Fmoc)-solid phase peptide synthesis (SPPS) [48]. (2) The sensitivity and selectivity of peptide probes can be further optimized by amino acid replacements [49]. (3) Peptide probes can be readily conjugated to appropriate solid support for further applications. (4) Peptide probes can be used in aqueous solution [50].

In this study, we focused on the development of short fluorescence peptide sensors for selective and sensitive detection of Zn^{2+}. For this purpose, we designed a new peptide with six amino acids and labeled it with a fluorescent dansyl group, i.e., Dansyl-His-Gln-Arg-Thr-His-Trp-NH_2 (D-P6). Fig. 1 shows the chemical structure of D-P6. It should be noted that the peptide sequence of His-Gln-Arg-Thr-His was based on a zinc finger peptide motif of CP1 (Pro-Tyr-Lys-Cys-Pro-Glu-Cys-Gly-Lys-Ser-Phe-Ser-Gln-Lys-Ser-Asp-Leu-Val-Lys-His-Gln-Arg-Thr-His-Thr-Gly), which was a consensus zinc finger peptide, as first designed by Krizek in 1991 [51]. A dansyl group and a Trp residue were further designed at the N- and C-terminus as an acceptor and a donor, respectively. As shown herein, the designed peptide probe exhibited a ratiometric response with a high selectivity to Zn^{2+}.

2. Experimental section

2.1. Chemicals

Peptide synthesis reagents Fmoc-His(Trt)-OH, Fmoc-L-Thr(tBu)-OH, Fmoc-L-Gln(Trt)-OH, Fmoc-L-Arg(Pbf)-OH, Fmoc-L-Trp(Boc)-OH, Rink Amide resin (0.66 mmol/g) were from C S Bio Co, USA. Dansyl Chloride was from Bio Basic Inc. Trifluoroacetic acid (TFA), diethyl ether, piperidine, 2-(1-H-benzotriazole-1yl)-1,1,3,3-tetramethyluronium hexafluorophosphate (HBTU), N,N-dimethylformamide (DMF), 1,2-Ethanedithiol (EDT, 98%), N,N-diisopropylethyl amine (DIEA), 4-(2-Hydroxyethyl)-1-piperazine ethanesulfonic acid (HEPES), Ethylenediaminetetraacetic acid disodium salt (EDTA) were of analytical grade. The metal ions stock solutions were prepared by dissolving $CdCl_2{\cdot}2.5H_2O$, $Zn(SO_4)_2{\cdot}7H_2O$, $CuCl_2{\cdot}2H_2O$, $CoCl_2{\cdot}6H_2O$, $Ni(NO_3)_2{\cdot}6H_2O$, $HgSO_4$, $AgNO_3$, Pb

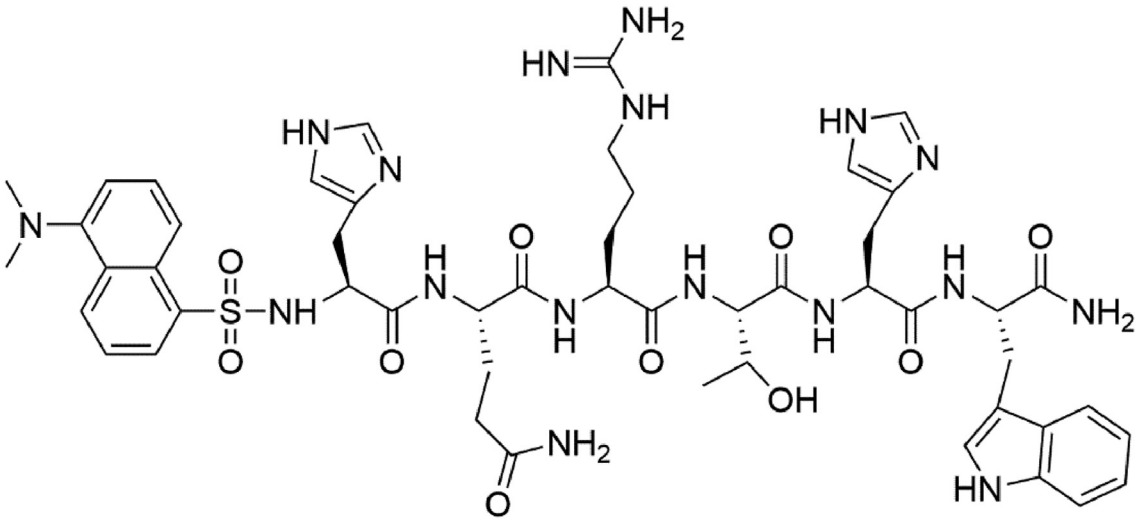

Fig. 1. Chemical structure of D-P6.

$(NO_3)_2$, $CaCl_2$, NaCl, $MnSO_4{\cdot}H_2O$, KCl, $MgSO_4{\cdot}7H_2O$, $BaCl_2{\cdot}2H_2O$, $CrCl_3{\cdot}6H_2O$, $AlCl_3{\cdot}6H_2O$ in double distilled water, respectively.

2.2. Peptide synthesis

The peptide with the sequence of Dansyl-His-Gln-Arg-Thr-His-Trp-NH_2 (D-P6) was synthesized on Rink Amide resin by standard Fmoc SPPS using a CS136 peptide synthesizer [52]. The dansyl group was coupled with the resin bound peptide by adding dansyl chloride (3 eq.) in DMF containing DIEA (3 eq.) and reacting for 1 h at room temperature. The crude peptide and all protecting groups were cleaved from the resin with TFA (82.5%) containing phenol (5%), thioanisole (5%), ethanedithiol (2.5%) and water (5%) for 3.5 h in dark place [53].

The solution was filtered in ice-cold ether and kept overnight, and then centrifuged. The resultant peptide was purified on Agilent 1200 HPLC system equipped with a Kromasil C18 column (250 × 4. 6 mm, 5 μm). Linear gradient was used for elution from 20% to 100% of eluent B in 30 min (eluents A: 0.1% CF_3COOH in H_2O, B: MeOH). The purity of the peptide was demonstrated with HPLC (**Fig. S1**) and ^{1}H NMR on a Bruker AVANCE NEO 500 MHz spectrometer. The peptide molecular mass (D-P6 calcd. 1096.2240; obsd. 1096.4979) was confirmed on LTQ ion-trap mass spectrometer (Thermo Fisher, San Jose, CA, USA) equipped with a nano-ESI source (**Fig. S2**).

2.3. Fluorescence measurements

Fluorescence emission spectra were recorded on Perkin-Elmer LS55 using rectangular quartz cuvette of 1.0 cm path length. The excitation wavelengths were set at 330 nm and 295 nm to measure dansyl fluorophore emission and Trp fluorophore emission, respectively [54,55]. The slit widths of excitation and emission were 10 nm and 5 nm, respectively. The fluorescence titration experiment of peptide was carried out by adding microliter aliquots of $ZnSO_4$ (1 mM stock solution) to freshly prepared peptide solutions in buffers (pH 7.4, 10 mM HEPES and 100 mM NaCl). Samples were equilibrated for 3 min before fluorescence measurement [56]. For the peptide selectively measurement, different kinds of metal ions including Cd^{2+}, Co^{2+}, Ni^{2+}, Cu^{2+}, Hg^{2+}, Pb^{2+}, Ag^{+}, Cr^{3+}, Ba^{2+}, Mg^{2+}, Ca^{2+}, Mn^{2+}, Na^{+}, Al^{3+} and K^{+} were used, and zinc salts consisting of different anions including SO_4^{2-}, Cl^{-}, ClO_4^{-} AcO^{-}, NO_3^{-} were also used for the impact on the detection. In addition, the binding reversibility of D-P6 to Zn^{2+} was studied by adding excess EDTA to the D-P6-Zn^{2+} system.

The fluorescence lifetime and quantum yield were carried out using FLS 1000 Photoluminescence Spectrometer (UK). The fitting formula for the fluorescence lifetime curve was given by the apparatus: $R(t) = B_1e^{(-t/\tau 1)} + B_2e^{(-t/\tau 2)}$. Fluorescence lifetime can be gotten by formula: $[\tau] = \Sigma\tau_iB_i$. The quality of the fit can be obtained by χ^2 value. In addition, we measured the fluorescence quantum yield of D-P6 in both the absence and presence of Zn^{2+}.

2.4. Determination of binding stoichiometry

The binding stoichiometry of peptide D-P6 with Zn^{2+} was determined by using Job's plot [57]. A series of solutions with varying mole fraction of Zn^{2+} was prepared while keeping the total concentration of peptide and Zn^{2+} at 20 μM. The fluorescence emission spectra were recorded from 310 to 570 nm at excited wavelength 295 nm or 400 to 640 nm at 330 nm, respectively. The binding stoichiometry was obtained by plotting a straight line through the maximum or minimum emission intensity in the titration curve. The association constant was estimated based on titration curve of D-P6 peptide with Zn^{2+}. Association constant was given by a nonlinear least squares fit of the data with the following equation [58].

$$y = \frac{x}{2 \times a \times b \times (1-x)^2} + \frac{x \times b}{2}$$

where x is the $I - I_0/I_{max} - I_0$, I is the fluorescence intensity at a particular concentration, I_0 is the fluorescence intensity of D-P6 without Zn^{2+}, I_{max} is the fluorescence intensity when all peptides of D-P6 is complexed with Zn^{2+}. Where a is the association constant and b is the concentration of D-P6, and y is the concentration of Zn^{2+}.

2.5. Molecular modeling studies

The initial structure of peptide His-Gln-Arg-Thr-His-Trp (P6) was obtained from the X-ray crystal structure of the designed zinc finger protein (PDB code 1MEY, molecule G) [59], and Trp was added to the C-terminus. A complex of 2P6-Zn^{2+} with a 2:1 ratio was constructed by using program VMD 1.9. The complex was then solvated in a cubic box of TIP3 water, which extended 10 Å away from any given protein atom. Counter ions (Na^+ and Cl^-) were further added to obtain the physiological ionic strength of 0.15 M by using the autoionize plug-in of VMD 1.9 [60]. The resulting system was minimized with NAMD2.9 (Nanoscale Molecular Dynamics) [61], using 5000 minimization steps with conjugate gradient method at 0 K, and equilibrated for 1,000,000 molecular dynamics steps (1 fs per step) at 300 K, then further minimized for 5,000 steps at 0 K. Visualization and data analysis were done with VMD 1.9.

2.6. ^{1}H NMR titration

^{1}H NMR titrations were carried out on a Bruker AVANCE NEO 500 MHz spectrometer in DMSO d_6/D_2O (30:70, v/v) and tetramethylsilane as an internal standard. The titrations were measured by keeping the concentration of D-P6 (3 mM) and varying the concentration of Zn^{2+} (0 mM, 0.75 mM, 1.5 mM and 3 mM) at room temperature.

2.7. Determination of the limit of detection

The limit of detection (LOD) of D-P6 to Zn^{2+} was calculated based on the fluorescence titration. In order to determine the S/N ratio, the fluorescence emission intensity of D-P6 was measured ten times and then the standard deviation of blank measurements was determined. Every average value of three times measurement of fluorescence intensity in the presence of different Zn^{2+} concentration was plotted versus Zn^{2+} concentration. The slope was obtained from this linear plot, and then the LOD value was calculated by the equation: $LOD = 3SD/m$, where SD presents the standard deviation of blank measurements, m presents the slop of the line.

2.8. UV and CD spectra measurements

UV absorption spectra and Circular dichroism (CD) spectra of D-P6 solutions were measured in pH 7.4, 10.0 mM HEPES buffer. UV absorption spectra were measured by Hitachi UH-4150 spectrophotometer. CD spectra were recorded on Jasco J-810 circular dichroism spectrophotometer over the wavelength of 200–300 nm with scanning speed at 200 nm/min using a 1 cm path length quartz optical cell.

2.9. Cell cytotoxicity of peptide and cell imaging

HeLa cells were cultured in DMEM supplemented with 10% FBS, streptomycin (100 μg/mL), penicillin (100 units mL^{-1}) and amphotericin B (250 μg/mL) at 37 °C in an atmosphere of 5% CO_2 and 95% air.

Cell viability was determined using the MTT assay. Cultured cells were seeded at a density of 1×10^4 cells per well in 96-well culture plates and incubated for 24 h. Different concentrations of L (10, 20, 40, 80 and 160 μM) were added to the 96- well culture plates, and cells were cultivated for another 24 h at 37 °C. Cell absorbance was measured by ELISA.

HeLa cells were seeded in glass bottomed dishes and cultured with 10 μM or 10 μM in the presence of 400 μM of Zn^{2+} for 30 min. All images were acquired using a Zeiss LSM 880 confocal microscope for fluorescence transmission, bright-field transmission and merged transmission respectively.

3. Results and discussion

3.1. Fluorescence spectra

Fluorescence emission spectra of D-P6 were measured in 10 mM HEPES buffer solution (pH 7.4) in the absence and presence of Zn^{2+} and was excited at a wavelength of 295 nm and 330 nm, respectively. Fig. 2**A** showed that when D-P6 was excited at 295 nm, two fluorescence peaks appeared at 519 nm and 362 nm, which correspond to the emission of dansyl group and Trp, respectively. With stepwise addition of Zn^{2+} to the solution of D-P6, the fluorescence emission intensity at 519 nm increased gradually, whereas the intensity changes at 362 nm revealed an opposite tendency. The fluorescence intensity ratio at 519 nm and 362 nm (F_{519}/F_{362}) increased from the original 1.5 to the final 12, accompanied by the moderate increase of Zn^{2+} concentration from 1.5 μM to 15 μM. This result showed that D-P6 produces a fluorescent resonance energy transfer (FRET) effect in the presence of Zn^{2+}, which suggests that D-P6 might fold upon binding of Zn^{2+}, with more close interactions between Trp and dansyl [62,63]. In case of the fluorescence emission spectra of D-P6 excited at 330 nm, only the emission peak of dansyl group at 519 nm was observed, as shown in Fig. 2**B**. With the stepwise addition of Zn^{2+} to the solution of D-P6, the fluorescence emission intensity at 519 nm increased gradually.

Fig. 3 is the fluorescence lifetime decay profiles for D-P6 and D-P6-Zn^{2+} solutions. It showed that the fluorescence lifetime of D-P6 was 2.47 ns at 362 nm emission, and the lifetime decreased to 2.28 ns (Fig. 3**A**) after binding with Zn^{2+}. Meanwhile, the lifetime of D-P6 was 4.78 ns at 519 nm emission, and the lifetime increased to 12.44 ns (Fig. 3**B**) under the same conditions. The fluorescence lifetime results are shown in Table 1, which also confirm a fluorescent resonance energy transfer.

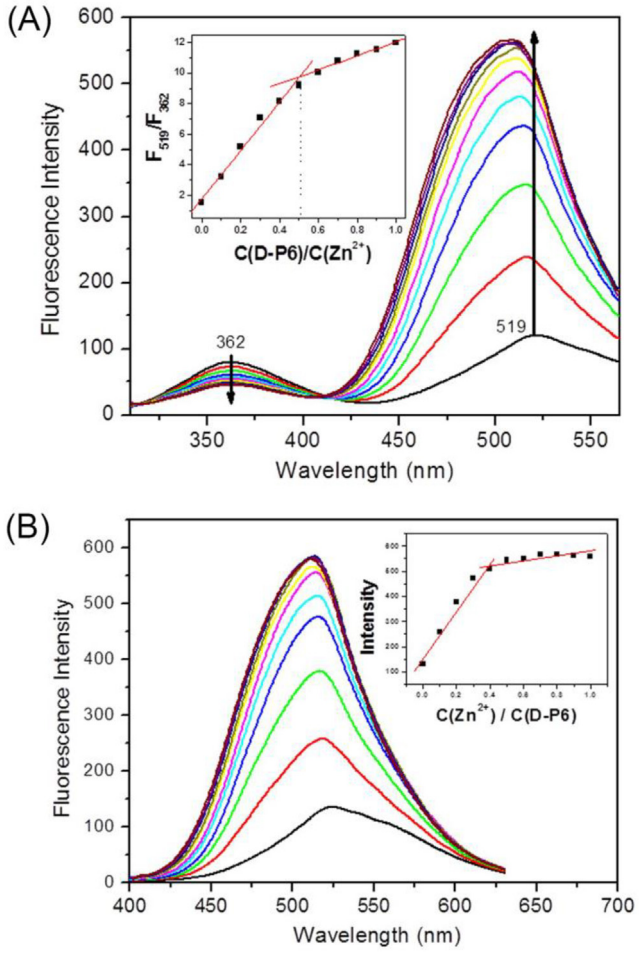

Fig. 2. Fluorescence emission spectra of D-P6 (15 μM) in 10 mM HEPES (100 mM NaCl, pH 7.4) in the absence and presence of Zn^{2+} (0, 1.5, 3, 4.5, 6, 7.5, 9, 10.5, 12, 13.5, 15 μM) with an excitation at (A) 295 nm and (B) 330 nm. Insets: (A) Titration curve based on the fluorescence emission ratio at 519 nm and 362 nm (F_{519}/F_{362}). (B) Ttitration curve based on the fluorescence emission at 519 nm.

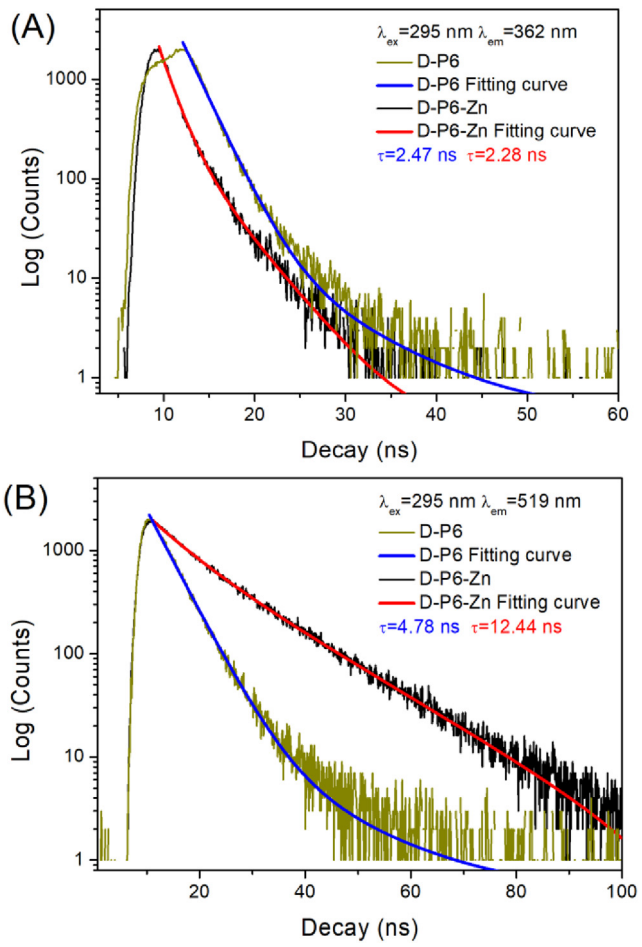

Fig. 3. Fluorescence lifetime decay profiles excited at 295 nm for D-P6 (15.0 μM) and D-P6-Zn (15.0 μM) in buffer (pH 7.4, 10 mM HEPES, 100 mM NaCl). (A) decay time at 362 nm emission; (B) decay time at 519 nm emission.

Table 1
Summary of fluorescence lifetime measurements in HEPES solutions.

Compounds	λ_{ex}	λ_{em}	τ [ns] (contribution, %)	χ^2
D-P6	295 nm	362 nm	τ_1 = 2.19 (95.04) τ_2 = 7.82 (4.96) τ = 2.47	1.218
D-P6-Zn	295 nm	362 nm	τ_1 = 1.47 (68.11) τ_2 = 4.00 (31.89) τ = 2.28	0.708
D-P6	295 nm	519 nm	τ_1 = 4.38 (96.24) τ_2 = 14.96 (3.76) τ = 4.78	1.046
D-P6-Zn	295 nm	519 nm	τ_1 = 6.70 (27.86) τ_2 = 14.66 (72.14) τ = 12.44	1.058

The fluorescence quantum yield of D-P6 was obtained in both the absence and presence of Zn^{2+} (**Fig. S3**). A quantum yield of 0.06 was obtained for D-P6 in the absence of Zn^{2+}. Following the addition of 1 equiv. of Zn^{2+}, the quantum yield increased to 0.17.

3.2. Binding stoichiometry, binding constant and the limit of detection

To investigate the binding stoichiometry of D-P6 for Zn^{2+}, we plotted the fluorescence emission spectral changes excited at both wavelengths (295 nm and 330 nm) versus the ratio of $c(Zn^{2+})/c$(D-P6). As shown in inset of Fig. 2, the titration curve indicated that a ratio of ~0.5 for $c(Zn^{2+})/c$(D-P6) was required for the saturation of the fluorescence emission intensity of D-P6, which suggests that the binding ratio of the peptide and Zn^{2+} was close to 2:1, forming a complex of $Zn(D\text{-}P6)_2$. Moreover, when excited at a wavelength of 330 nm (Fig. 2B, inset), the plot of the intensity of fluorescence versus the ratio of $c(Zn^{2+})/c$(D-P6) also suggested that a complex of $Zn(D\text{-}P6)_2$ was presumably formed upon Zn^{2+} binding to D-P6.

In addition, we investigated the coordination stoichiometry between D-P6 and Zn^{2+} using Job's plot. As shown in Fig. 4, it showed a maximum peak at 0.34 mol fraction of Zn^{2+}, indicating that the binding stoichiometry between D-P6 and Zn^{2+} was 2:1, which agrees well with the result from the titration curves (Fig. 2, insets).

To evaluate the binding affinity of D-P6 for Zn^{2+}, we calculated the association constant (K_a) based on the fluorescence titration curve. As shown in **Fig. S4**, the fluorescence intensity at 519 nm increased and reached a saturation state when the Zn^{2+} concentration reached ~7.5 μM. Therefore, the K_a value of D-P6 for Zn^{2+} can be calculated by 2:1 complex model for D-P6-Zn^{2+} system by using nonlinear least-squares fit analysis of the emission intensity, which was calculated to be (9.0 ± 0.32) × 10^{12} M^{-2}, indicating a high binding affinity of D-P6 for Zn^{2+}. This is likely due to the strong coordination interactions between the imidazole groups of the His residues and Zn^{2+} in the complex of $Zn(D\text{-}P6)_2$.

With the gradual addition of Zn^{2+}, the fluorescence emission intensity increased and reached the plateau region within 1 min, which suggested that the D-P6 could detect Zn^{2+} rapidly. Therefore, the limit of detection of Zn^{2+} can be derived from the linear relationship between the emission intensity and Zn^{2+} concentration. **Fig. S5** depicted a linear increase of the emission intensity accompanied by the concentration of Zn^{2+} (R^2 = 0.9907). The emission intensity at 519 nm increased proportionately with the increasing of concentration of Zn^{2+} when the concentration of Zn^{2+} was less than 2 μM, and the limit of detection was calculated to be 33 nM.

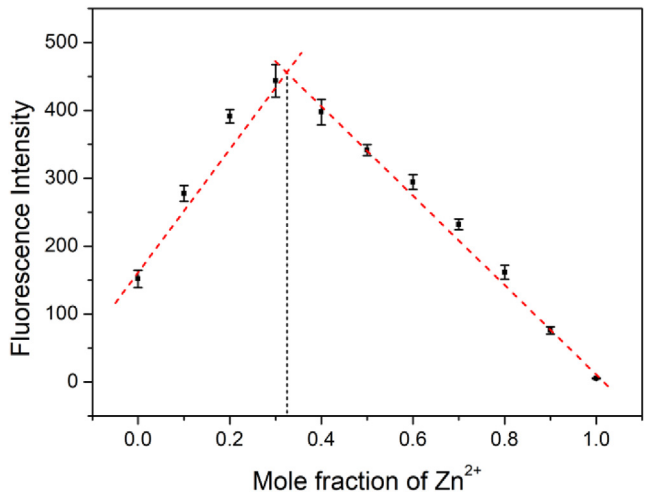

Fig. 4. Job's plot for D-P6 with Zn^{2+} in 10 mM HEPES buffer solution (pH 7.4), the total concentration of D-P6 and Zn^{2+} was 20 μM.

3.3. The effects of pH, time and temperature

Additionally, we investigated the effect of solution pH on the D-P6 and D-P6-Zn^{2+} systems by performing pH titration. As shown in **Fig. S6**, at pH < 5, both D-P6 and D-P6-Zn^{2+} systems showed a very low value of F_{519}/F_{362} ratio. The result indicated that the addition of Zn^{2+} has no influence on the fluorescence emission of D-P6 in this condition. This is probably due to the protonation of dimethylamino group ($pK_a \approx 4$) of dansyl fluorophore. Besides, histidine cannot coordinate to Zn^{2+} at pH less than 6 due to the protonation of its imidazole group. Thus, D-P6 showed no spectral change in the presence of Zn^{2+}. In the pH range from 6 to 9, D-P6 exhibited a sensitive turn on response to Zn^{2+}, with ~5-fold enhancement in the F_{519}/F_{362} ratio. Note that the F_{519}/F_{362} ratio of D-P6-Zn^{2+} system slightly decreased at pH > 9. Accordingly, D-P6 is sensitive to Zn^{2+} and can thus be used for the detection of Zn^{2+} in the moderate basic conditions (pH 7–9).

In addition, we investigated the influence of temperature and time on D-P6 toward Zn^{2+}. **Fig. S7** illustrates the effect of D-P6 on the detection of Zn^{2+} at different temperatures. The fluorescence intensity ratio of D-P6-Zn^{2+} (F_{519}/F_{362}) decreased with the increase of temperature, which may be caused by the inactivation of some D-P6 at high temperature. The overall results showed that D-P6 can detect Zn^{2+} in a wide temperature range. **Fig. S8** illustrates the time kinetic study of D-P6-Zn^{2+} in 10 mM HEPES buffer. Within one minute, the binding of D-P6 toward Zn^{2+} caused the fluorescence ratio signal (F_{519}/F_{362}) to reach its maximum. The results show that D-P6 has a fast response ability to detect Zn^{2+}.

3.4. Modeling structure of 2P6-Zn^{2+}-complex

In order to provide structural information for the peptide binding to Zn^{2+}, we performed a molecular modeling and

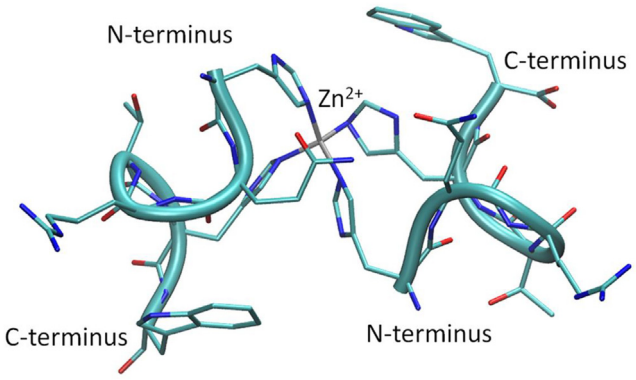

Fig. 5. Modeling structure of 2P6-Zn^{2+} complex, showing the coordination of zinc ion (grey ball) by four His residues from two monomers.

dynamic simulation study. Based on the X-ray structure of the designed zinc finger protein (PDB code 1MEY) [59], we constructed the initial structure of the peptide, His-Gln-Arg-Thr-His-Trp (P6), and then its dimer (termed 2P6) with Zn^{2+} ion by using the program VMD. The four His residues were then patched to the zinc ion and molecular dynamic simulation was performed by using the program NAMD. As shown in Fig. 5, the α-helical structure of peptide was well retained upon binding to the Zn^{2+} ion. Both His residues from the monomer coordinated to the metal ion, with an average Nε-Zn distance of ~1.9 Å in agreement with that in the X-ray structure (1.83–1.87 Å), which results in a tetrahedral conformation for the zinc metal center. These observations suggest that D-P6 presumably binds Zn^{2+} ion and forms a 2:1 complex.

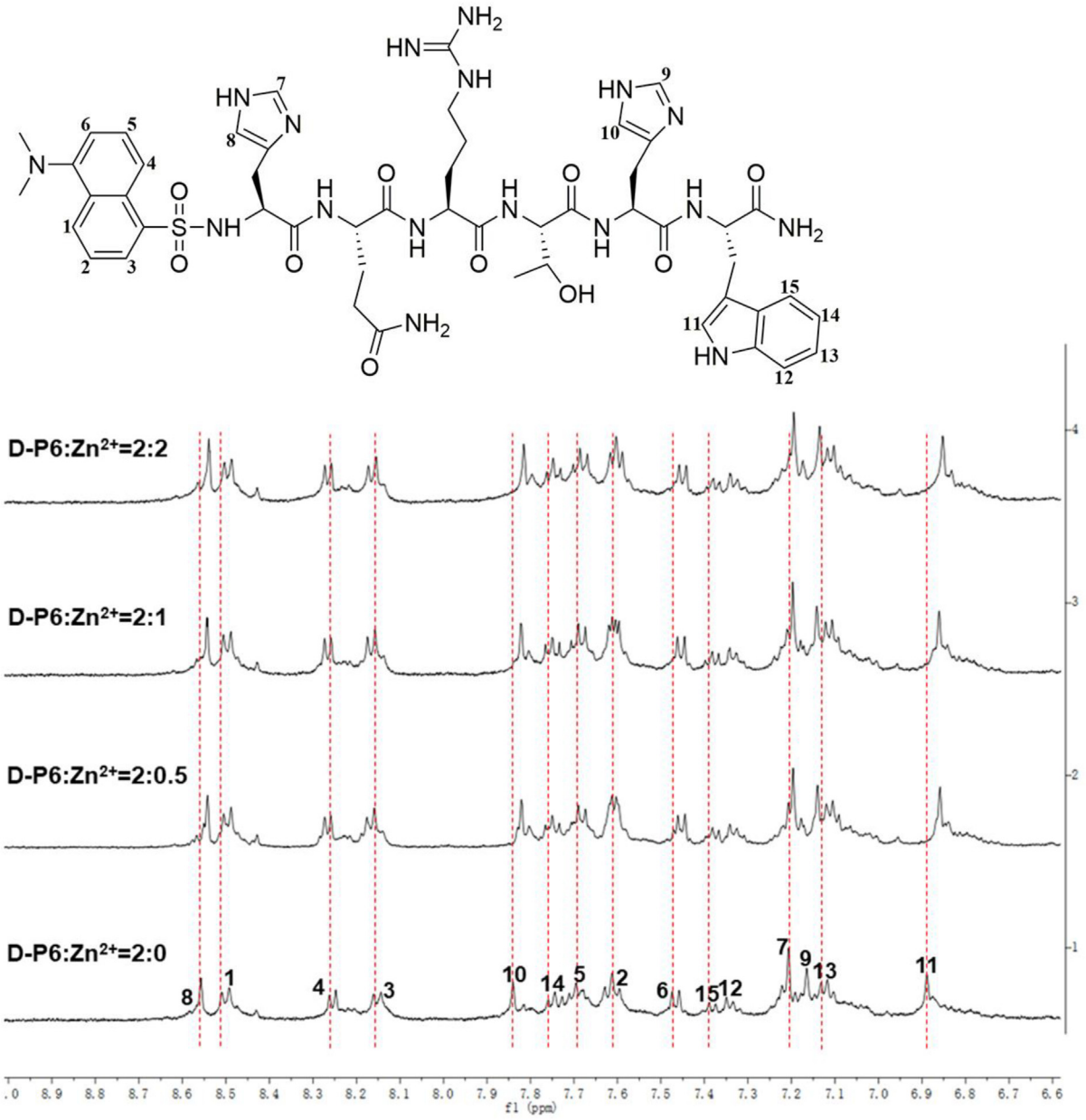

Fig. 6. Partial ^{1}H NMR titration spectra of D-P6 in the absence and presence of Zn^{2+} in DMSO d_6/D_2O (30:70, v/v).

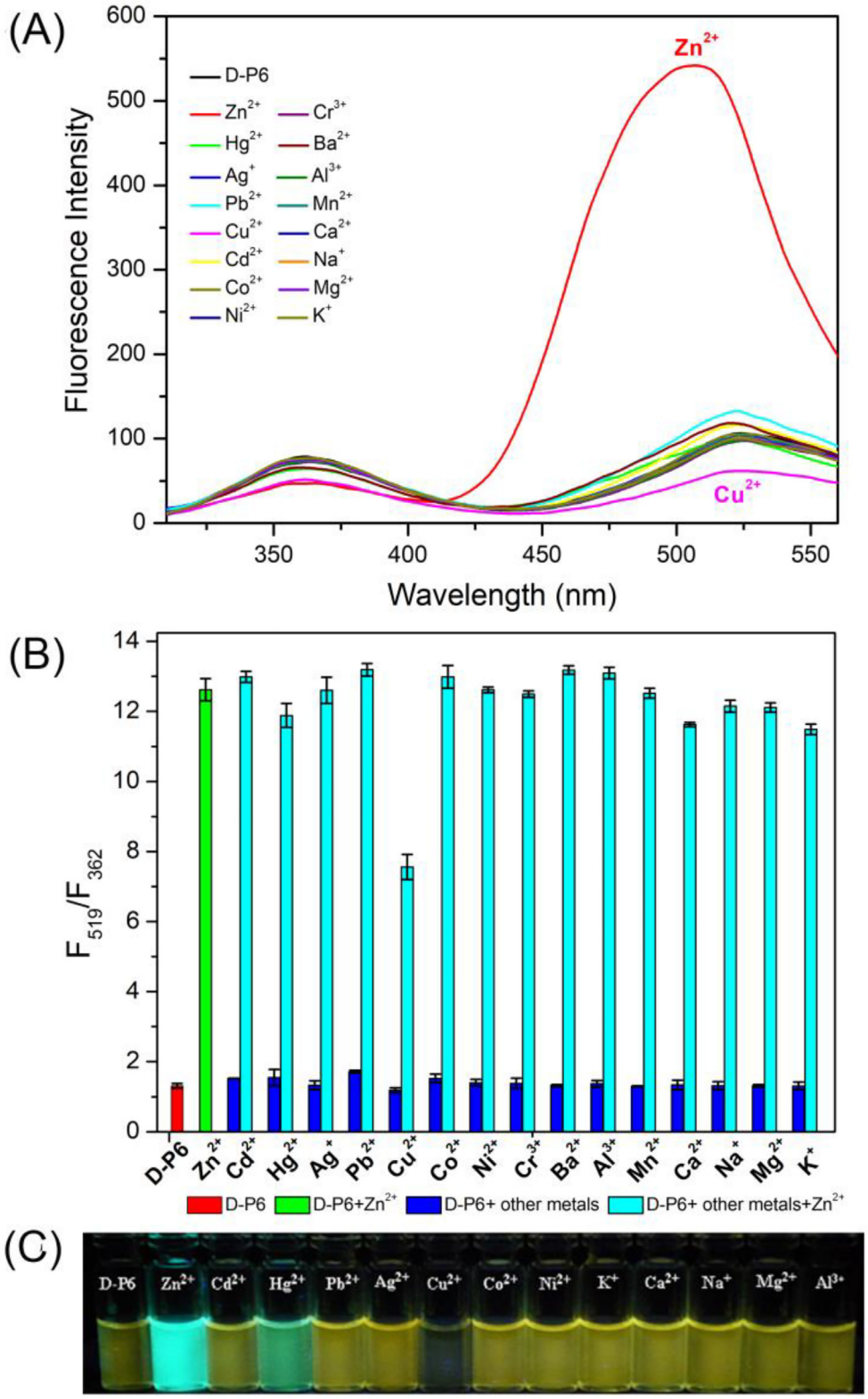

Fig. 7. (A) Fluorescence spectra of 15 μM D-P6 in the presence of various metal ions in 10 mM HEPES (100 mM NaCl, pH 7.4). (B) Fluorescence responses of 15 μM D-P6 to various metal ions in 10 mM HEPES (100 mM NaCl, pH 7.4), λ_{ex} = 295 nm. Bars represent the final fluorescence intensity ratio at 519 nm to 362 nm (F_{519}/F_{362}), and blue bars represent the addition of 1 eq. of metal ions (1000 eq. for Na^+, Ca^{2+}, K^+ and Mg^{2+}) to a 15 μM D-P6 solution and cyan bars represent the subsequent addition of 1 eq. of Zn^{2+} to the solution. (C) Visible emission of 50 μM D-P6 with 1 eq. various metal ions observed in 10 mM HEPES buffer solutions.

3.5. ^1H NMR spectra

^1H NMR experiments can provide further information about the interactions between D-P6 and Zn^{2+}. Fig. 6 showed the partial ^1H NMR titration spectra of D-P6 with Zn^{2+} in DMSO d_6/D_2O (30:70, v/v). When Zn^{2+} was added, chemical shifts were observed for H(7) and H(8) in the His imidazole group nearing the dansyl group, which indicate that the Zn^{2+} ion coordinates to an imidazole group. The shifts of the aromatic protons of the dansyl moiety, H(1)-H(6), suggested that Zn^{2+} may interact with the dansyl moiety of D-P6, as suggested by a dansylamide-fantionalized cyclen probe in previous study [64]. In addition, both H(9) and H(10) in the second His residue next to the tryptophan showed chemical shifts. Furthermore, H(11–15) in tryptophan exhibited chemical shifts with varying degrees, which may be caused by changes in the microenvironment after the coordination of D-P6 with Zn^{2+}. The results showed that the dansyl-His moiety may act as a bidentate ligand to form a 2:1 (2D-P6:Zn^{2+}) complex. At the same time, a 2:1 binding mode may also be formed by two histidines as ligands, whereas it might be affected by the pH value.

When the concentration of Zn^{2+} increased to a ratio of 1:1 (D-P6:Zn^{2+}), the ^1H NMR signals of H(9) and H(10) shifted to a high-field compared with a ratio of 2:1 (2D-P6:Zn^{2+}), whereas the peak of H(2) of the dansyl moiety returned almost to the original position of D-P6. From these observations, it can be inferred that at higher Zn^{2+} concentrations, the second His was more likely to participate in the coordination with Zn^{2+} to form a 1:1 complex. These results further suggest that D-P6 bound to Zn^{2+} mainly with a ratio of 2:1, and it can also be a ratio of 1:1 with a higher Zn^{2+} concentration.

3.6. Evaluation of selectivity

We further evaluated the fluorescence response selectivity of D-P6 for Zn^{2+} by comparing with the fluorescence responses of D-P6 to various metal ions in 10 mM HEPES buffer (pH 7.4). Fig. 7**A** showed the fluorescence emission spectra of 15 μM D-P6 (λ_{ex} = 295-nm) in the presence of various metal ions (1 eq.). The most dramatic increase in intensity of fluorescence spectra of D-P6 was observed in the presence of Zn^{2+}, whereas other metal ions had no significant effects, indicating a high selectivity of D-P6 for Zn^{2+}.

Moreover, to confirm the high selectivity of D-P6-Zn^{2+} over other metal ions, we carried out competition experiments in the presence of 1 eq. of Co^{2+}, Ni^{2+}, Ba^{2+}, Al^{3+}, Mn^{2+}, Cu^{2+}, Cd^{2+}, Cr^{3+}, Ag^{+}, Hg^{2+}, Pb^{2+} and 1000 eq. of Na^{+}, K^{+}, Mg^{2+}, Ca^{2+}, Na^{+}, with subsequent addition of 1 eq. of Zn^{2+}. As shown in Fig. 7**B**, the fluorescence emission ratio F_{519}/F_{362} of the D-P6-Zn^{2+} system was unperturbed in the presence of these metal ions, indicating the strongest affinity and highest selectivity for Zn^{2+}. It is notable that the addition of Zn^{2+} to these solutions induced an immediate increase of the ratio F_{519}/F_{362} of D-P6-Zn^{2+} except in Cu^{2+} solution. Notably, the ratio of D-P6-Zn^{2+} system showed nearly 10-fold of D-P6 in the presence of other metal ions. These results confirmed that D-P6 is sensitive to Zn^{2+}, which thus makes it applicable in the design of a Zn^{2+} sensor.

Fig. 7**C** presents the color changes of the D-P6 solution in the absence and presence of Zn^{2+} and other ions excited by a wavelength of 365 nm. It showed a light green color in D-P6 solution containing Zn^{2+}. Fluorescence color of D-P6 solution changed from yellow to olive by addition of Hg^{2+}. Moreover, D-P6 solution containing Cu^{2+} was colorless, whereas the D-P6 solution containing other metal ions did not show color changes.

Similarly, we also investigated the effects of different anions on the fluorescence property of the system under the same condition. As shown in **Fig. S9**, when adding zinc salts consisting of different anions to the D-P6 solution, there were no obvious changes on the fluorescence ratio F_{519}/F_{362} of D-P6, indicating that these anions have no interference to the detection of Zn^{2+}.

In addition, to determine whether the binding of D-P6 to Zn^{2+} is reversible, we added an excessive of EDTA to D-P6-Zn^{2+} solution. The result showed that the spectrum of D-P6-Zn^{2+} returned to an initial level of the Zn^{2+}-free solution, which demonstrates the reversibility of the signaling mechanism of the peptide (**Fig. S10**).

3.7. UV and CD spectra of the D-P6-Zn^{2+} system

Upon the addition of 0–1 equiv. Zn^{2+} solutions, the UV titration spectra revealed that the absorbances of D-P6 at 220 nm, 250 nm, 280 nm and 330 nm gradually decreased (**Fig. S11**), showing that interaction between D-P6 and Zn^{2+} occurred. The molar absorption coefficients at 280 nm (tryptophan residue) and at 330 nm (Dansyl group) were reduced from 6.3×10^3 $M^{-1}\cdot cm^{-1}$, 3.2×10^3 $M^{-1}\cdot cm^{-1}$ to 5.2×10^3 $M^{-1}\cdot cm^{-1}$, 2.9×10^3 $M^{-1}\cdot cm^{-1}$, respectively. From the absorption spectra changes, we can infer that D-P6 may chelate with Zn^{2+} *via* the sulfonamide group of the dansyl fluorophore and side chain group of the amino acid residues.

Circular dichroism (CD) spectroscopy is often used to analyze the conformational changes of biomolecules. The CD spectrum of D-P6 contains two negative absorption bands at 227 and 250 nm. After the addition of Zn^{2+}, the negative absorption peaks at 227 and 250 nm decreased significantly (**Fig. S12**). It suggested that D-P6 interacted with Zn^{2+}, leading to a large change in the conformation of D-P6.

3.8. Cytotoxicity and intracellar fluorescence imaging

HeLa cells were chosen to evaluate the cytotoxicity of the sensor using MTT assay. As shown in Fig. 8, with the concentration of peptide D-P6 from 10 μM to 160 μM, the cell survival rate exceeded 95%. These results confirmed that the sensor exhibits a low toxicity to the cells even at a high concentration, which suggests that the peptide has the potentiality to be used for the Zn^{2+} detection in living cells.

Additionally, confocal microscopy experiment was employed to evaluate the ability of the sensor as an imaging tool in living cells. The HeLa cells were incubated with 20 μM peptide for 30 min at 37 °C. All images were taken with a Zeiss LSM 880 confocal microscope with excitation at 405 nm and emission at 550 nm. HeLa cells did not show fluorescence in the absence of peptide (Fig. 9A1–3). As shown in Fig. 9B1–3, HeLa cells displayed light flu-

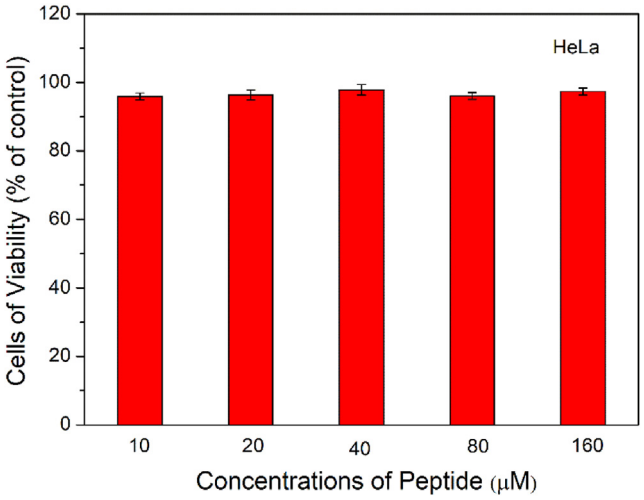

Fig. 8. MTT assay of peptide D-P6 with a concentration from 10 μM to 160 μM.

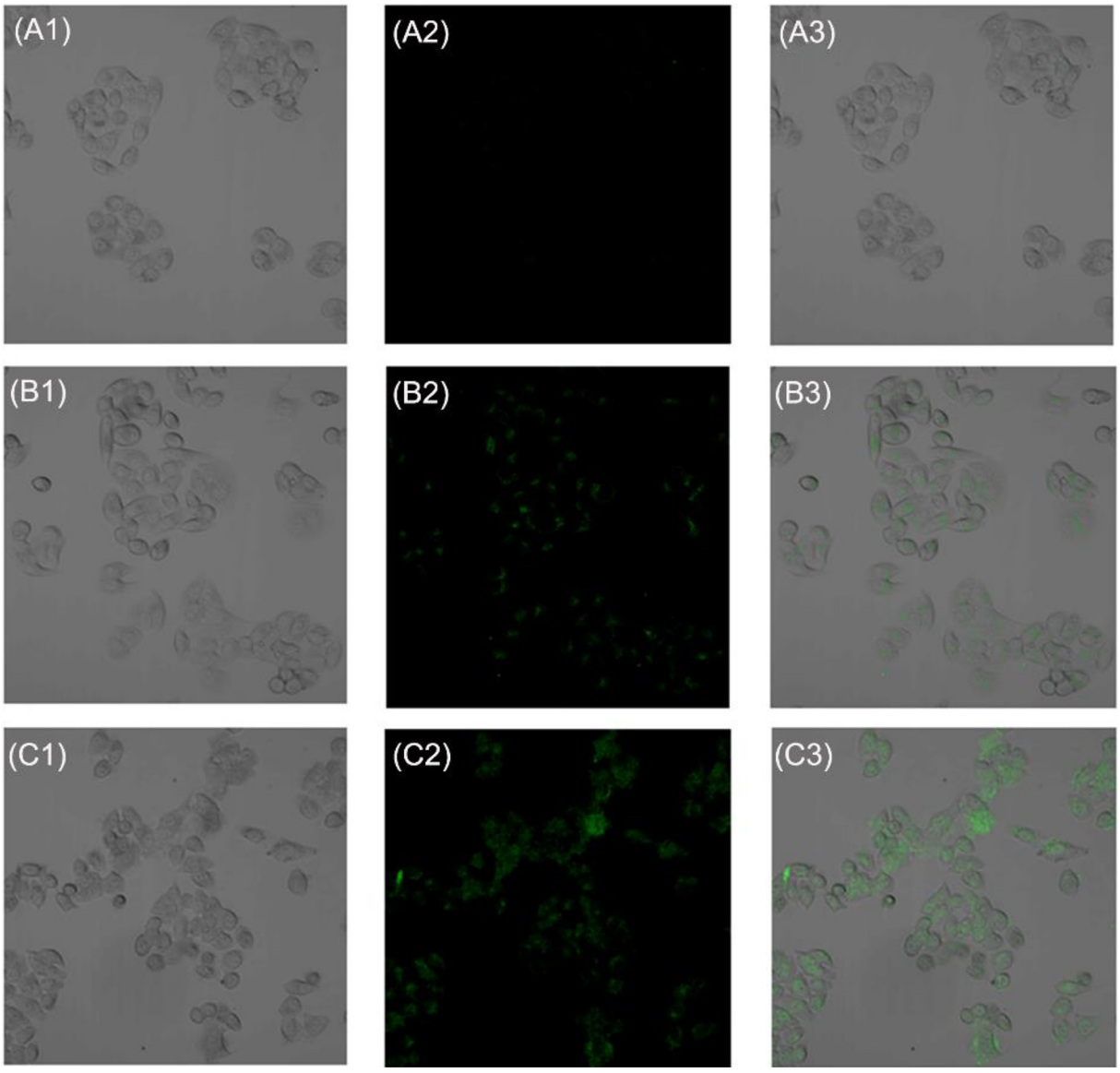

Fig. 9. Fluorescence images of living HeLa cells with excitation at 405 nm and emission at 550 nm. (A) Living HeLa cells. (B) Cells incubated with 10 μM peptide for 30 min. (C) Cells incubated with 10 μM peptide for 30 min and subsequently treated with 400 μM Zn^{2+} for another 30 min. Bright-field transmission images (A1, B1, C1), fluorescent-field transmission images (A2, B2, C2), merged transmission images (A3, B3, C3).

orescence after incubation with 10 μM peptide, indicating the penetration of the peptide in the cells. After the addition of 400 μM Zn^{2+} to the cells, the fluorescence intensity of the intracellular region enhanced remarkably, as shown in Fig. 9C1–3. Therefore, these observations indicate that the peptide can penetrate the HeLa cells and respond to the intracellular Zn^{2+} subsequently.

4. Conclusion

In this study, we designed and synthesized a new fluorescent peptide, Dansyl-His-Gln-Arg-Thr-His-Trp-NH_2, by Fmoc solid-phase peptide synthesis method. This peptide exhibited a high affinity for Zn^{2+} compared to other metal ions, presumably formed a 2:1 (peptide/Zn^{2+}) complex at substoichiometric amounts of Zn^{2+}, as suggested by spectroscopic studies and molecular modeling. Furthermore, at equimolar Zn^{2+} concentration the peptide might form a 1:1 complex. Based on this property, we developed a highly selective and sensitive Zn^{2+} ratiometric fluorescent sensor in aqueous solutions, by utilizing the fluorescent resonance energy transfer effect between Trp residue and fluorophore dansyl group. In addition, the sensor displayed a very low biotoxicity, which was successfully used for detection of Zn^{2+} in living HeLa cells, suggesting potential applications in biological science.

CRediT authorship contribution statement

Shuaibing Yu: Investigation, Formal analysis, Data curation, Writing - original draft. **Yan Li:** Investigation, Formal analysis, Data curation, Writing - original draft. **Lei Gao:** Investigation, Formal analysis. **Peiran Zhao:** Investigation. **Lei Wang:** Formal analysis. **Lianzhi Li:** Conceptualization, Validation, Writing - review & editing, Supervision. **:** . **Ying-Wu Lin:** Software, Visualization, Writing - review & editing, Supervision.

Declaration of Competing Interest

The authors declare that they have no known competing financial interests or personal relationships that could have appeared to influence the work reported in this paper.

Acknowledgments

This project was supported by the Scientific Research Foundation of Liaocheng University, China (No. 318011919) and the National Natural Science Foundation of China (21974068).

Appendix A. Supplementary material

Supplementary data to this article can be found online at https://doi.org/10.1016/j.saa.2021.120042.

References

[1] G.K. Andrews, Cellular zinc sensors: MTF-1 regulation of gene expression, Biometals 14 (2001) 223–237.
[2] S.C. Burdette, S.J. Lippard, Meeting of the minds: Metalloneurochemistry, Proc. Natl. Acad. Sci. USA 100 (2003) 3605–3610.
[3] J. Silva, R. Williams, The biological chemistry of the elements: The inorganic chemistry of life, Biochem. Educ. 20 (1992) 62–63.
[4] C.J. Frederickson, J.Y. Koh, A.I. Bush, The neurobiology of zinc in health and disease, Nat. Rev. Neurosci. 6 (2005) 449–462.
[5] P.J. Fraker, L.E. King, Reprogramming of the immune system during zinc deficiency, Annu. Rev. Nutr. 24 (2004) 277–298.
[6] A.I. Bush, W.H. Pettingell, G. Multhaup, M. Paradis, J.P. Vonsattel, J.F. Gusella, K. Beyreuther, C.L. Masters, R.E. Tanzi, Rapid induction of alzheimer a beta amyloid formation by zinc, Science 265 (1994) 1464–1467.
[7] J.Y. Koh, S.W. Suh, B.J. Gwag, Y.Y. He, C.Y. Hsu, D.W. Choi, The role of zinc in selective neuronal death after transient global cerebral ischemia, Science 265 (1996) 1013–1016.
[8] C.F. Walker, R.E. Black, Zinc and the risk for infectious disease, Annu. Rev. Nutr. 24 (2004) 255–275.
[9] E. Callender, K.C. Rice, The urban environmental gradient: Anthropogenic influences on the spatial and temporal distributions of lead and zinc in sediments, Environ. Sci. Technol. 34 (2000) 232–238.
[10] A. Voegelin, S. Pfister, A.C. Scheinost, M.A. Marcus, R. Kretzschmar, Changes in zinc speciation in field soil after contamination with zinc oxide, Environ. Sci. Technol. 39 (2005) 6616–6623.
[11] G. Hennrich, H. Sonnenschein, U. Resch-Genger, Redox switchable fluorescent probe selective for either Hg(II) or Cd(II) and Zn(II), J. Am. Chem. Soc. 121 (1999) 5073–5074.
[12] E.M. Nolan, S.J. Lippard, Tools and tactics for the optical detection of mercuric ion, Chem. Rev. 108 (2008) 3443–3480.
[13] S. Malashikhin, N.S. Finney, Fluorescent signaling based on sulfoxide profluorophores: Application to the visual detection of the explosive TATP, J. Am. Chem. Soc. 130 (2008) 12846–12847.
[14] S. Mizukami, R. Takikawa, F. Sugihara, M. Shirakawa, K. Kikuchi, Dual-function probe to detect protease activity for fluorescence measurement and ^{19}F MRI, Angew. Chem. Int. Edit. 48 (2009) 3641–3643.
[15] R. Guliyev, A. Coskun, E.U. Akkaya, Design strategies for ratiometric chemosensors: Modulation of excitation energy transfer at the energy donor site, J. Am. Chem. Soc. 131 (2009) 9007–9013.
[16] C.S. Lim, D.W. Kang, Y.S. Tian, J.H. Han, H.L. Hwang, B.R. Cho, Detection of mercury in fish organs with a two-photon fluorescent probe, Chem. Commun. 46 (2010) 2388–2390.
[17] J.F. Callan, A.P. de Silva, D.C. Magri, Luminescent sensors and switches in the early 21st century, Tetrahedron 61 (2005) 8551–8588.
[18] K. Rurack, Flipping the light switch 'ON' – the design of sensor molecules that show cation-induced fluorescence enhancement with heavy and transition metal ions, Spectrochim. Acta A 57 (2001) 2161–2195.
[19] A.W. Czarnik, Chemical communication in water using fluorescent chemosensors, Acc. Chem. Res. 27 (1994) 302–308.
[20] H.N. Kim, M.H. Lee, H.J. Kim, J.S. Kim, J. Yoon, A new trend in rhodamine-based chemosensors: Application of spirolactam ring-opening to sensing ions, Chem. Soc. Rev. 37 (2008) 1465–1472.
[21] Z.C. Xu, K.H. Baek, H.N. Kim, J.N. Cui, X.H. Qian, D.R. Spring, I. Shin, J.Y. Yoon, Zn^{2+}-triggered amide tautomerization produces a highly Zn^{2+}-selective, cell-permeable, and ratiometric fluorescent sensor, J. Am. Chem. Soc. 132 (2010) 601–610.
[22] E.L. Que, D.W. Domaille, C.J. Chang, Metals in neurobiology: Probing their chemistry and biology with molecular imaging, Chem. Rev. 108 (2008) 1517–1949.
[23] K. Kuroda, M. Ueda, Molecular design of the microbial cell surface toward the recovery of metal ions, Curr. Opin. Biotech. 22 (2011) 427–433.
[24] P. Carol, S. Sreejith, A. Ajayaghosh, Ratiometric and near-infrared molecular probes for the detection and imaging of zinc ions, Chem.–Asian J. 2 (2007) 338–348.
[25] H. Wang, Q. Gan, X. Wang, L. Xue, S. Liu, H. Jiang, Small molecular fluorescent sensor with femtomolar sensitivity for zinc ion, Org. Lett. 9 (2007) 4995–4998.
[26] K. Kiyose, H. Kojima, Y. Urano, T. Nagano, Development of a ratiometric fluorescent zinc ion probe in near-infrared region, based on tricarbocyanine chromophore, J. Am. Chem. Soc. 128 (2006) 6548–6549.
[27] K. Komatsu, K. Kikuchi, H. Kojima, Y. Urano, T. Nagano, Selective zinc sensor molecules with various affinities for Zn^{2+}, revealing dynamics and regional distribution of synaptically released Zn^{2+} in hippocampal slices, J. Am. Chem. Soc. 127 (2005) 10197–10204.
[28] K. Komatsu, Y. Urano, H. Kojima, T. Nagano, Development of an iminocoumarin-based zinc sensor suitable for ratiometric fluorescence imaging of neuronal zinc, J. Am. Chem. Soc. 129 (2007) 13447–13454.
[29] J. Wan, W. Duan, K. Chen, Y. Tao, J. Dang, K. Zeng, Y. Ge, J. Wu, D. Liu, Selective and sensitive detection of Zn(II) ion using a simple peptide-based sensor, Sensor. Actuat. B-Chem. 255 (2018) 49–56.
[30] P. Wang, D. Zhou, B. Chen, High selective and sensitive detection of Zn(II) using tetrapeptide-based dansyl fluorescent chemosensor and its application in cell imaging, Spectrochim. Acta A 204 (2018) 735–742.
[31] P. Wang, J. Wu, Highly Selective and sensitive detection of Zn(II) and Cu(II) ions using a novel peptide fluorescent probe by two different mechanisms and its application in live cell imaging, Spectrochim. Acta A 208 (2019) 140–149.
[32] G. Donadio, R.D. Martino, R. Oliva, L. Petraccone, P.D. Vecchio, B.D. Luccia, E. Ricca, R. Isticato, A.D. Donato, E. Notomista, A new peptide-based fluorescent probe selective for zinc(II) and copper(II), J. Mater. Chem. B 4 (2016) 6979–6988.
[33] P. Wang, J. Wu, P. Su, C. Shan, P. Zhou, Y. Ge, D. Liu, W. Liu, Y. Tang, A novel fluorescent chemosensor based on tetra-peptides for detecting zinc ions in aqueous solutions and live cells, J. Mater. Chem. B 4 (2016) 4526–4533.
[34] S. Yu, Z. Wang, X. Pang, L. Wang, L. Li, Y. Lin, Peptide-based metal ion sensors, Prog. Chem. 33 (2021) 380–393.
[35] H.-X. Wang, C.-W. Wei, X.-J. Wang, H.-F. Xiang, X.-Z. Yang, G.-L. Wu, Y.-W. Lin, A facile gelator based on phenylalanine derivative is capable of forming fluorescent Zn-metallohydrogel, detecting Zn^{2+} in aqueous solutions and imaging Zn^{2+} in living cells, Spectrochim. Acta A 250 (2021) 119378.
[36] C. Lu, Z. Xu, J. Cui, R. Zhang, X. Qian, Ratiometric and highly selective fluorescent sensor for cadmium under physiological pH range: A new strategy to discriminate cadmium from zinc, J. Org. Chem. 72 (2007) 3554–3557.
[37] L. Xue, C. Liu, H. Jiang, Highly sensitive and selective fluorescent sensor for distinguishing cadmium from zinc ions in aqueous media, Org. Lett. 11 (2011) 1655–1658.
[38] L. Xue, Q. Liu, H. Jiang, Ratiometric Zn^{2+} fluorescent sensor and new approach for sensing Cd^{2+} by ratiometric displacement, Org. Lett. 11 (2011) 3454–3457.
[39] H. Zhu, J. Fan, B. Wang, X. Peng, Fluorescent, MRI, and colorimetric chemical sensors for the first-row d-block metal ions, Chem. Soc. Rev. 44 (2015) 4337–4366.
[40] G. Klein, D. Kaufmann, S. Schurch, J.L. Reymond, A fluorescent metal sensor based on macrocyclic chelation, Chem. Commun. 561 (2001) 561–562.
[41] L. Prodi, M. Montalti, N. Zaccheroni, F. Dallavalle, G. Folesani, M. Lanfranchi, R. Corradini, S. Pagliari, R. Marchelli, Dansylated polyamines as fluorescent sensors for metal ions: Photophysical properties and stability of copper(II) complexes in solution, Helv. Chim. Acta 84 (2001) 690–706.
[42] X. Pang, J. Dong, L. Gao, L. Wang, S. Yu, J. Kong, L. Li, Dansyl-peptide dual-functional fluorescent chemosensor for Hg^{2+} and biothiols, Dyes Pigments 173 (2020) 107888.
[43] X. Pang, L. Wang, L. Gao, H. Feng, J. Kong, L. Li, Multifunctional peptide-based fluorescent chemosensor for detection of Hg^{2+}, Cu^{2+} and S^{2-} ions, Luminescence 34 (2019) 585–594.
[44] Z. Wang, H. Feng, Y. Li, T. Xu, Z. Xue, L. Li, A high selective fluorescent ratio sensor for Cd^{2+} based on the interaction of peptide with metal ion, Chinese J. Inorg. Chem. 31 (2015) 1946–1952.
[45] Y. Li, L. Li, X. Pu, G. Ma, E. Wang, J. Kong, Z. Liu, Y. Liu, Synthesis of a ratiometric fluorescent peptide sensor for the highly selective detection of Cd^{2+}, Bioorg. Med. Chem. 22 (2012) 4014–4017.
[46] X. Pang, L. Gao, H. Feng, X. Li, J. Kong, L. Li, A peptide-based multifunctional fluorescent probe for Cu^{2+}, Hg^{2+} and biothiols, New J. Chem. 42 (2018) 15770–15777.
[47] H. Feng, L. Gao, X. Ye, L. Wang, Z. Xue, J. Kong, L. Li, Synthesis of a heptapeptide and its application in the detection of mercury(II) ion, Chem. Res. Chin. Univ. 33 (2017) 155–159.
[48] R.B. Merrifield, Solid phase peptide synthesis. I. the synthesis of a tetrapeptide, J. Am. Chem. Soc. 85 (1963) 2149–2154.
[49] B. Wang, H. Li, Y. Gao, H. Zhang, Y. Wu, A multifunctional fluorescence probe for the detection of cations in aqueous solution: The versatility of probes based on peptides, J. Fluoresc. 21 (2011) 1921–1931.
[50] B.P. Joshi, J.W. Park, W.I. Lee, K.H. Lee, Ratiometric and turn-on monitoring for heavy and transition metal ions in aqueous solution with a fluorescent peptide sensor, Talanta 78 (2009) 903–909.
[51] B.A. Krizek, B.T. Amann, V.J. Kilfoil, D.L. Merkle, J.M. Berg, A consensus zinc finger peptide: Design, high-affinity metal binding, a pH-dependent structure, and a His to Cys sequence variant, J. Am. Chem. Soc. 113 (1991) 4518–4523.
[52] L.N. Neupane, P. Thirupathi, S.J. Jang, M.J. Jang, J.H. Kim, K.H. Lee, Highly selectively monitoring heavy and transition metal ions by a fluorescent sensor based on dipeptide, Talanta 85 (2011) 1566–1574.
[53] G.B. Fields, R.L. Nobel, ChemInform abstract: Solid phase peptide synthesis utilizing 9-fluorenylmethoxycarbonylamino acids, Int. J. Pept. Protein Res. 35 (1990) 161–214.
[54] J.M. Kim, C.R. Lohani, L.N. Neupane, Y. Choi, K.H. Lee, Highly sensitive turn-on detection of Ag^{+} in aqueous solution and live cells with a symmetric fluorescent peptide, Chem. Commun. 48 (2012) 3012–3014.

[55] P. Wang, J. Wu, P. Zhou, W. Liu, Y. Tang, A novel peptide-based fluorescent chemosensor for measuring zinc ions using different excitation wavelengths and application in live cell imaging, J. Mater. Chem. B 3 (2015) 3617–3624.
[56] P.F. Muhlradt, M. Kieß, H. Meyer, R. Sußmuth, G. Jung, Structure elucidation, and synthesis of a macrophage stimulatory lipopeptide from mycoplasma fermentans acting at picomolar concentration, J. Exp. Med. 185 (1997) 1951–1958.
[57] A.R. Reddi, T.R. Guzman, R.M. Breece, D.L. Tierney, B.R. Gibney, Deducing the energetic cost of protein folding in zinc finger proteins using designed metallopeptides, J. Am. Chem. Soc. 129 (2007) 12815–12827.
[58] L.N. Neupane, J.Y. Park, J.H. Park, K.H. Lee, Turn-on fluorescent chemosensor based on an amino acid for Pb(II) and Hg(II) ions in aqueous solutions and role of tryptophan for sensing, Org. Lett. 15 (2013) 254–257.
[59] C.A. Kim, J.M. Berg, A 2.2 Å resolution crystal structure of a designed zinc finger protein bound to DNA, Nat. Struct. Biol. 3 (1996) 940–945.
[60] W. Humphrey, A. Dalke, K. Schulten, VMD: Visual molecular dynamics, J. Mol. Graph. 14 (1996) 33–38.
[61] L. Kalé, R. Skeel, M. Bhandarkar, R. Brunner, A. Gursoy, N. Krawetz, J. Phillips, A. Shinozaki, K. Varadarajan, K. Schulten, NAMD2: Greater scalability for parallel molecular dynamics, J. Comp. Phys. 151 (1999) 283–312.
[62] Y. Zheng, X. Cao, J. Orbulescu, V. Konka, F.M. Andreopoulos, S.M. Pham, R.M. Leblanc, Peptidyl fluorescent chemosensors for the detection of divalent copper, Anal. Chem. 75 (2003) 1706–1712.
[63] Y. Zhao, Z. Zhong, Detection of Hg^{2+} in aqueous solutions with a foldamer-based fluorescent sensor modulated by surfactant micelles, Org. Lett. 8 (2006) 4715–4717.
[64] T. Koike, T. Watanabe, S. Aoki, E. Kimura, M. Shiro, A novel biomimetic zinc(II)-fluorophore, dansylamidoethyl-pendant macrocyclic tetraamine 1,4,7,10-tetraazacyclododecane (Cyclen), J. Am. Chem. Soc. 118 (1996) 12696–12703.